Quantification of Anthocyanins and Flavonols in Milk-Based Food Products by Ultra Performance Liquid Chromatography-Tandem Mass Spectrometry

ARTICLE *in* ANALYTICAL CHEMISTRY · AUGUST 2009

Impact Factor: 5.64 · DOI: 10.1021/ac900608g · Source: PubMed

5 AUTHORS, INCLUDING:

Kornél Nagy
Nestlé S.A.
42 PUBLICATIONS **753** CITATIONS
SEE PROFILE

Karine Redeuil
Nestlé S.A.
13 PUBLICATIONS **150** CITATIONS
SEE PROFILE

Martin Kussmann
Nestlé Institute of Health Sciences S.A.
104 PUBLICATIONS **2,187** CITATIONS
SEE PROFILE

Anal. Chem. **2009,** *81,* 6347–6356

Quantification of Anthocyanins and Flavonols in Milk-Based Food Products by Ultra Performance Liquid Chromatography−Tandem Mass Spectrometry

Kornél Nagy,*,† Karine Redeuil,† Raymond Bertholet,‡ Heike Steiling,§ and Martin Kussmann†

Functional Genomics and Nutrient Bioavailability Groups, BioAnalytical Science Department, and Bioactives and Micronutrients, Food Science and Technology Department, Nestlé Research Centre, Nestec Ltd., Lausanne, Switzerland

The present article describes the development and validation of an ultra performance liquid chromatography−tandem mass spectrometry (UPLC−MS/MS) method for the comprehensive quantification of anthocyanin and flavonol constituents of milk-based food products. Protein precipitation by acidified methanol and ultrafiltration was utilized as sample preparation to preserve overall polyphenol composition but to eliminate milk proteins in order to comply with UPLC. Reversed-phase chromatography was optimized to achieve separation of 27 analytes in 10 min in order to reduce suppression effects, achieve a wide dynamic range, and most importantly, to resolve isomeric compounds. Positive-ion electrospray mass spectrometric detection and fragmentation of analytes was optimized, final transitions were selected for maximized selectivity, reliable quantification, and reduction of false positives. The quantitative performance of the method was validated, the main features include (1) range of lower limits of detection 0.3−30 ng/mL for glycosylated analytes, 10−300 ng/mL for aglycones, (2) lower limits of quantification 1−100 ng/mL for glycosylated analytes, 30−1 000 ng/mL for aglycones, (3) averaged intraday precision 9%, (4) calibrated range 2−180 000 ng/mL for glycosylated analytes, 60−600 000 ng/mL for aglycones, and (5) averaged accuracy 101%. Applications for yogurt and ice cream products are given. The presented data suggest that this method will help to better characterize the polyphenol composition of milk-based food products for quality control, for assessment of dietary intake, and for polyphenol bioavailability/bioefficacy studies.

Anthocyanins and other flavonols are promising dietary components for the nutritional prevention and management of several health disorders.[1] Their bioavailability and bioefficacy are studied more and more frequently to better understand their health-beneficial action at the molecular level. Anthocyanins were reported to inhibit the growth of different cancer cell lines,[2] and flavonoids were found to decrease the number of immobilized leukocytes during reperfusion, suggesting anti-inflammatory action.[3] Tsuda reported that anthocyanins are even promising dietary components for weight management, since they can ameliorate adipocyte function.[4] While several polyphenols were associated with health benefits, their bioavailability and bioefficacy can be dramatically different even among structural isomers.[5,6] This latter fact underlines the need for detailed characterization of polyphenol content and bioavailability in dietary interventions and highlights the importance of selective, sensitive, and comprehensive analytical approaches.

Anthocyanins are polyphenolic phytochemicals with structures comprising an anthocyanidin aglycone and different sugar moieties, see Figure 1. They are commonly found in many plants, and their most common dietary sources are berries such as currants.[7,8] However, the polyphenol composition varies dramatically between fruits.[9] Major anthocyanins in red raspberry have been identified as cyanidin and pelargonidin glycosylated with rutinose and sophorose,[10] whereas cyanidin 3-*O*-glucoside and pelargonidin 3-*O*-glucoside are predominant in strawberry.[11] Blackberry anthocyanins have been characterized as only cyanidin-based compounds.[12,13] A literature survey also reveals that the

* To whom correspondence should be addressed. Kornél Nagy, Nestlé Research Centre, Vers-Chez-les-Blanc, 1000 Lausanne, Switzerland. E-mail: kornel.nagy@rdls.nestle.com. Phone: + 41 21 785 8290. Fax: + 41 21 785 9486.
† Functional Genomics Group, BioAnalytical Science Department.
‡ Bioactives and Micronutrients, Food Science and Technology Department.
§ Nutrient Bioavailability Group, BioAnalytical Science Department.

(1) Seeram, N. P. *J. Agric. Food Chem.* **2008**, *56*, 627–629.
(2) Zhang, Y. J.; Seeram, N. P.; Lee, R.; Feng, L.; Heber, D. *J. Agric. Food Chem.* **2008**, *56*, 670–675.
(3) Friesenecker, B.; Tsai, A. G.; Allegra, C.; Intaglietta, M. *Int. J. Microcirc. Clin. Exp.* **1994**, *14*, 50–55.
(4) Tsuda, T. *J. Agric. Food Chem.* **2008**, *56*, 642–646.
(5) Donovan, J. L.; Crespy, V.; Oliveria, M.; Cooper, K. A.; Gibson, B. B.; Williamson, G. *Free Radical Res.* **2006**, *40*, 1029–34.
(6) Schroeter, H.; Heiss, C.; Balzer, J.; Kleinbongard, P.; Keen, C. L.; Hollenberg, N. K.; Sies, H.; Kwik-Uribe, C.; Schmitz, H. H.; Kelm, M. *Proc. Natl. Acad. Sci. U.S.A.* **2006**, *103*, 1024–1029.
(7) Maatta-Riihinen, K. R.; Kamal-Eldin, A.; Torronen, A. R. *J. Agric. Food Chem.* **2004**, *52*, 6178–6187.
(8) Maatta, K. R.; Kamal-Eldin, A.; Torronen, A. R. *J. Agric. Food Chem.* **2003**, *51*, 6736–6744.
(9) Mullen, W.; Marks, S. C.; Crozier, A. *J. Agric. Food Chem.* **2007**, *55*, 3148–57.
(10) Beattie, J.; Crozier, A.; Duthie, G. G. *Curr. Nutr. Food Sci.* **2005**, *1*, 71–86.
(11) Aaby, K.; Ekeberg, D.; Skrede, G. *J. Agric. Food Chem.* **2007**, *55*, 4395–4406.
(12) Fan-Chiang, H. J.; Wrolstad, R. E. *J. Food Sci.* **2005**, *70*, C198–C202.
(13) Stintzing, F. C.; Stintzing, A. S.; Carle, R.; Wrolstad, R. E. *J. Agric. Food Chem.* **2002**, *50*, 396–99.

10.1021/ac900608g CCC: $40.75 © 2009 American Chemical Society
Published on Web 07/10/2009

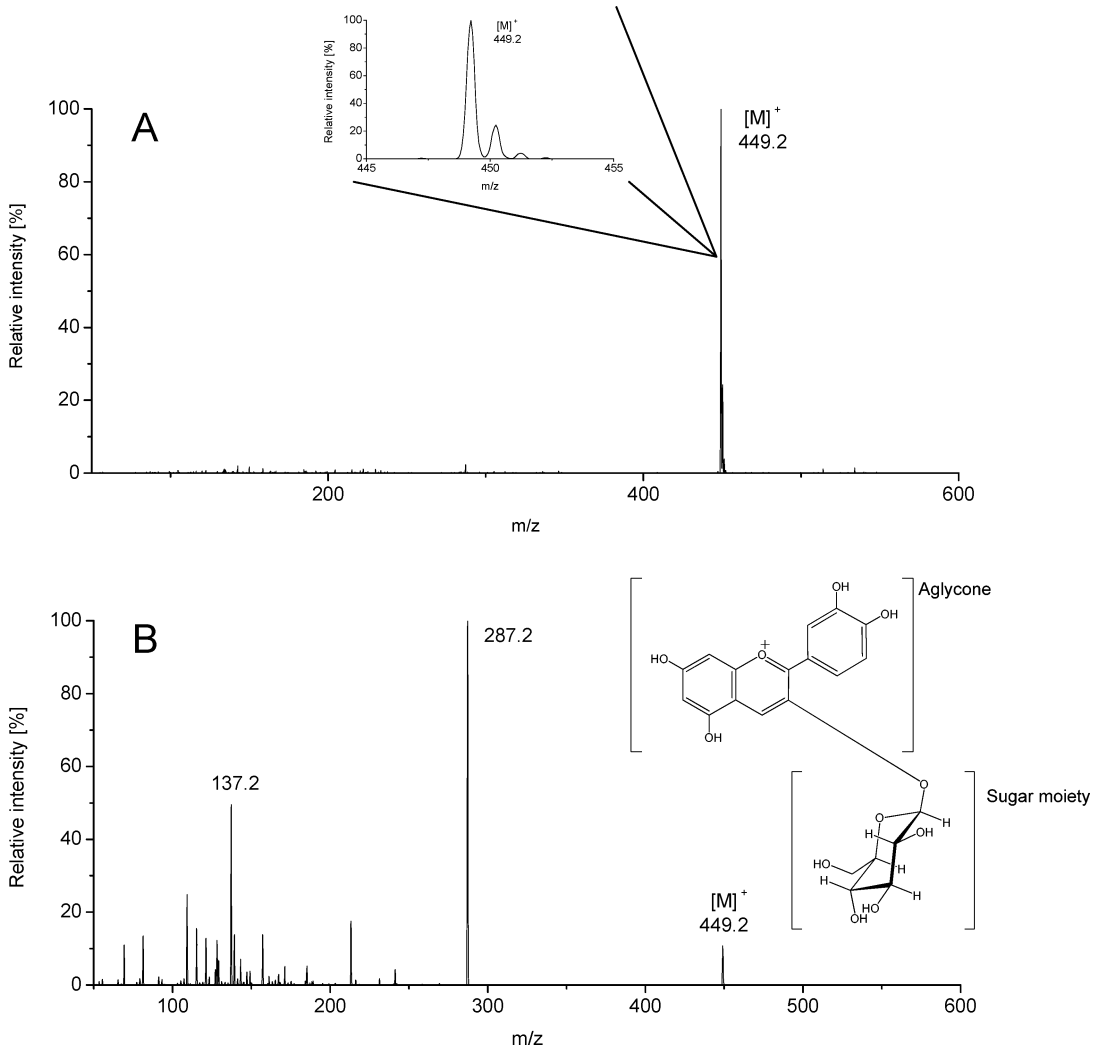

Figure 1. Single stage electrospray mass spectrum of cyanidin 3-*O*-glucoside in positive-ion mode (A). The spectrum is strongly dominated by the molecular ion $[M]^+$, and no significant in-source fragmentation was observed. The insert depicts the magnified isotope pattern of the molecular ion. Panel B shows, the tandem mass spectrum of cyanidin 3-*O*-glucoside. The fragmentation pattern was obtained by varying the collision energy between 5 and 50 V. The spectrum is dominated by the fragment that resulted from the loss of the sugar moiety. As an example for anthocyanin structure, cyanidin 3-*O*-glucoside is depicted in the insert.

reported anthocyanin content of different berries varies among publications emphasizing the need for more selective, accurate, and comprehensive analytical methodologies. Moreover, for nutritional intervention studies, the mere knowledge of berry type is not sufficient: the knowledge of exact anthocyanin composition of the applied food is imperative.

It has been also reported that even different varieties of the same fruit (for instance anthocyanins from different grape,[14,15] currant,[8] or apricot[16] varieties) exhibit a significantly different anthocyanin profile. For example while in table grapes peonidin 3-*O*-glucoside is the most abundant anthocyanin, the latter was found to be malvidin 3-*O*-glucoside in wine grape varieties.[15] Isolation and structural characterization of phenolics including anthocyanins was reported by Amberlite XAD16-resin and C_{18} columns, HPLC−UV−VIS, HPLC−Couloarray,[11] and nuclear magnetic resonance (NMR) spectroscopy methods.[2]

A wide range of analytical methods have been reported for profiling anthocyanin content of fruits. The common approach combines liquid chromatography based separation with light absorbance based quantification[8,9,14−20,20−23] usually at 520 nm wavelength. LC−UV−VIS was also reported for controlling the

(14) Kammerer, D.; Claus, A.; Carle, R.; Schieber, A. *J. Agric. Food Chem.* **2004**, *52*, 4360–4367.
(15) Cantos, E.; Espin, J. C.; Tomas-Barberan, F. A. *J. Agric. Food Chem.* **2002**, *50*, 5691–5696.
(16) Ruiz, D.; Egea, J.; Gil, M. I.; Tomas-Barberan, F. A. *J. Agric. Food Chem.* **2005**, *53*, 9544–9552.
(17) Mertz, C.; Cheynier, V.; Gunata, Z.; Brat, P. *J. Agric. Food Chem.* **2007**, *55*, 8616–8624.
(18) Mullen, W.; Edwards, C. A.; Serafini, M.; Crozier, A. *J. Agric. Food Chem.* **2008**, *56*, 713–719.
(19) Nielsen, I. L. F.; Haren, G. R.; Magnussen, E. L.; Dragsted, L. O.; Rasmussen, S. E. *J. Agric. Food Chem.* **2003**, *51*, 5861–5866.
(20) Aaby, K.; Wrolstad, R. E.; Ekeberg, D.; Skrede, G. *J. Agric. Food Chem.* **2007**, *55*, 5156–5166.
(21) Kahle, K.; Kraus, M.; Scheppach, W.; Ackermann, M.; Ridder, F.; Richling, E. *Mol. Nutr. Food Res.* **2006**, *50*, 418–23.
(22) Nicoue, E. E.; Savard, S.; Belkacemi, K. *J. Agric. Food Chem.* **2007**, *55*, 5626–5635.
(23) Chaovanalikit, A.; Wrolstad, R. E. *J. Food Sci.* **2004**, *69*, C73–C83.
(24) Hager, A.; Howard, L. R.; Prior, R. L.; Brownmiller, C. *J. Food Sci.* **2008**, *73*, H134–H140.

Table 1. Applied UPLC Gradient Parameters for the Elution of Anthocyanins

time [min]	solvent A [%]	solvent B [%]	flow rate [μL/min]	curve value
0	100	0	400	1
5	91	9	400	6
7	85	15	400	6
8	0	100	400	6
10	0	100	400	6
10.1	100	0	400	6
13	100	0	400	1

degradation of anthocyanins during processing and storage.[24] Tandem mass spectrometry was reported to characterize anthocyanin content of fruit extract mostly by Paul traps[8,11,14,18] (3D-traps) or rarely by triple quadrupole instruments.[25] In these cases, the purpose of mass spectrometric analysis was to confirm the identity of the analytes by studying their fragmentation patterns as described by Montoro et al.[26] and Tian et al.[25] Until now, none of the published papers described tandem mass spectrometry based quantification of anthocyanins and validation of such methodology in fruit or milk-based food products.

In this article we describe a combination of ultrafiltration and ultra performance liquid chromatography−tandem mass spectrometry (UPLC−MS/MS) as a method for quantification of anthocyanins and flavonols in milk-based food formulations. This method is proposed to characterize dietary anthocyanin intake in human bioavailability and bioefficacy trials.

EXPERIMENTAL SECTION

Chemicals. HPLC grade water, methanol, and acetonitrile were obtained from Chemie Brunschwig AG, Basel, Switzerland. LC−MS grade formic acid and ammonium acetate were from Fluka/Sigma-Aldrich Chemie GmbH, Buchs, Switzerland. Polyphenol standards were purchased either from Polyphenols Laboratories AS, Sandnes, Norway, or from Extrasynthese, Genay, France. Stable isotope labeled cyanidin 3-*O*-$^{13}C_6$-glucoside was purchased from Orphachem S.A. Clermont-Ferrand, France. Ultrafiltration tubes (Millipore Amicon Ultra 4, 3 kDa) were purchased from Millian, Geneva, Switzerland.

Standard Solutions. Commercially available standards were individually weighted and dissolved in pure methanol or DMSO for ellagic acid. These starting solutions were used to prepare stock solutions A (mix of 20 compounds) and B (mix of 7 compounds), for composition see Table 2. Stock solutions A and B were further diluted (by methanol or methanol/formic acid 9:1 depending on the applied solvent in the extraction step) to obtain the final spiking solutions in order to achieve the desired spiking levels for calibration.

Internal standard cyanidin 3-*O*-$^{13}C_6$-glucoside was dissolved in pure methanol to obtain a 100 μg/mL stock solution. This stock solution was further diluted to obtain a 1 μg/mL working solution in pure methanol or methanol/formic acid 9:1. This 1 μg/mL working solution was used to achieve a 20 ng/mL internal standard level in the extracting solvent at the start of the sample preparation process.

(25) Tian, Q. G.; Konczak, I.; Schwartz, S. J. *J. Agric. Food Chem.* **2005**, *53*, 6503–6509.

(26) Montoro, P.; Tuberoso, C. I. G.; Perrone, A.; Piacente, S.; Cabras, P.; Pizza, C. *J. Chromatogr., A* **2006**, *1112*, 232–240.

Table 2. Composition of Stock Solutions A and B Used for Calibration Purposes

analyte number	analyte	concentration in stock solution [μg/mL]	solution
1	cyanidin	120	B
2	cyanidin 3-*O*-arabinoside	72	A
3	cyanidin 3-*O*-galactoside	12	A
4	cyanidin 3-*O*-glucoside	12	A
5	cyanidin 3-*O*-rutinoside	120	A
6	cyanidin 3-*O*-sophoroside	36	A
7	delphinidin	400	B
8	delphinidin 3-*O*-glucoside	120	A
9	delphinidin 3-*O*-rutinoside	120	A
10	ellagic acid	400	B
11	kaempferol	180	A
12	kaempferol 3-*O*-glucoside	180	A
13	malvidin	36	B
14	malvidin 3-*O*-glucoside	72	A
15	myricetin	6	B
16	pelargonidin	540	A
17	pelargonidin 3-*O*-glucoside	36	A
18	peonidin	540	A
19	peonidin 3-*O*-arabinoside	54	A
20	peonidin 3-*O*-galactoside	36	A
21	peonidin 3-*O*-glucoside	72	A
22	petunidin	1200	B
23	petunidin 3-*O*-glucoside	72	A
24	quercetin	12	B
25	quercetin 3-*O*-galactoside	360	A
26	quercetin 3-*O*-rhamnoside	600	A
27	quercetin 3-*O*-rutinoside	360	A

Sample Preparation. A volume of 0.5 mL of sample was pipetted into an amber Pyrex 15 tube, and 2 mL of methanol (containing 20 ng/mL internal standard) was added. The mixture was vortexed for 15 s and stored at − 20 °C for 1 h to allow proteins to precipitate. Then the tubes were centrifuged at 3000*g* (3950 rpm) for 5 min at 4 °C in a Sigma 3-16K centrifuge. The supernatant was transferred into ultrafiltration tubes (3 kDa cutoff) that were then kept at −20 °C, and the remaining precipitate was mixed with additional 2 mL of a methanol/formic acid 9:1 mixture (containing 20 ng/mL internal standard). The resulting acidic mixture was vortexed for 15 s and stored at −20 °C for 1 h to allow the proteins to precipitate. Then tubes were centrifuged again at 3000*g* (3950 rpm) for 5 min at 4 °C. Finally, this acid supernatant was combined with the previous neutral extract, and the resulting 4 mL of solution was centrifuged at 3893*g* (4500 rpm) for 30 min at 20 °C. The filtrates were either stored in the freezer or immediately evaporated under nitrogen flow. Before analysis, samples were reconstituted in a 500 μL mixture of 5 mM ammonium acetate/0.5% formic acid (containing 2 mg/mL ascorbic acid), centrifuged at 2000*g* (3225 rpm) for 5 min at 4 °C, and transferred into amber vials for analysis. A volume of 10 μL was injected into the UPLC−MS/MS system.

Preparation of Spiked Samples for Calibration. The method of standard additions was used to obtain the calibration for each analyte. This calibration method was selected in order to correct/ascertain matrix effects occurring during sample preparation (recovery, saturation effects) and analysis (suppression). To construct the calibration curves, samples were enriched by known amounts of analytes using standard solutions A and B as described above.

Preparation of Skimmed Milk Powder Samples. Skimmed milk powder was used to mimic the matrix of milk-based food

Table 3. Experimental Parameters of UPLC−MS/MS for the Detection of Anthocyanins and Flavonols

analyte	average molecular weight [Da]	Q1 *m/z*	Q3 *m/z*	retention time [min]	cone voltage [V]	collision energy [V]	function start [min]	function
cyanidin	287.3	287.1	137.0	5.65	50.0	20.0	4.8	7.3
cyanidin 3-*O*-arabinoside	419.4	419.1	287.1	4.05	35.0	20.0	3	5.8
cyanidin 3-*O*-galactoside	449.4	449.1	287.1	3.38	35.0	20.0	2.5	5
cyanidin-3-*O*-glucoside	449.4	449.1	287.1	3.80	35.0	20.0	2.5	5
cyanidin 3-*O*-rutinoside	595.5	595.1	287.1	4.20	45.0	30.0	3.5	6
cyanidin 3-*O*-sophoroside	611.5	611.1	287.1	3.44	45.0	40.0	2.6	5.1
delphinidin	303.3	303.1	229.0	4.35	50.0	20.0	3	5.2
delphinidin 3-*O*-glucoside	465.4	465.1	303.1	3.12	40.0	20.0	1.5	4
delphinidin 3-*O*-rutinoside	611.5	611.1	303.1	3.46	45.0	40.0	2.6	5.1
ellagic acid	302.2	303.1	229.0	4.67	60.0	30.0	3.5	6.8
kaempferol	286.2	287.1	153.0	7.88	50.0	30.0	7.2	9.6
kaempferol 3-*O*-glucoside	448.4	449.1	287.1	6.73	25.0	10.0	5.2	8.5
malvidin	331.3	331.1	287.0	7.57	50.0	20.0	6.7	9.2
malvidin 3-*O*-glucoside	493.5	493.1	331.1	5.62	35.0	20.0	4	7
myricetin	318.2	319.1	153.0	6.25	50.0	30.0	5.5	7.9
pelargonidin	271.3	271.1	121.0	6.76	50.0	30.0	5.9	8.3
pelargonidin 3-*O*-glucoside	433.4	433.1	271.1	4.51	30.0	20.0	3	6.2
peonidin	301.3	301.1	286.0	7.30	50.0	20.0	6.5	9
peonidin 3-*O*-arabinoside	433.4	433.1	301.1	5.41	30.0	20.0	4.5	7
peonidin 3-*O*-galactoside	463.4	463.1	301.1	4.64	35.0	20.0	3.8	6.8
peonidin 3-*O*-glucoside	463.4	463.1	301.1	5.14	35.0	20.0	3.8	6.8
petunidin	317.3	317.1	203.0	6.25	50.0	20.0	5.5	7.9
petunidin 3-*O*-glucoside	479.5	479.1	317.1	4.39	35.0	20.0	3.3	6.2
quercetin	302.3	303.1	153.0	7.74	50.0	30.0	7	9.5
quercetin 3-*O*-galactoside	464.4	465.1	303.1	5.21	30.0	15.0	4.5	7.2
quercetin 3-*O*-rhamnoside	448.4	449.1	303.1	6.55	30.0	10.0	5.9	8.2
quercetin 3-*O*-rutinoside	610.5	611.1	303.1	5.67	30.0	20.0	4.8	7.5

products. For the purpose, 10 g of skimmed milk powder was dispersed into 100 mL of pure water. The solution was then gently agitated using a magnetic stirrer for 1 h at room temperature. Finally, the solution was kept at 4 °C until use.

Liquid Chromatography. UPLC separation of anthocyanins and flavonols was achieved on a C18 column (Acquity BEH, 1.7 μm, 50 mm × 2.1 mm, Waters, 186002350) at room temperature using a Waters Acquity UPLC system. Mobile phase A was water/formic acid 9:1 mixture, mobile phase B was 100% acetonitrile. The mobile phase gradient is summarized in Table 1. An eλ-Acquity photodiode array was used as the UV−VIS detector prior to connection to the mass spectrometer. The detector was operated in a 190−800 nm wavelength range at a 20 point/s rate at 1.2 nm resolution.

Mass Spectrometry. Mass spectrometric detection was performed on a Waters Quattro Premier XE triple quadrupole tandem mass spectrometer in positive electrospray (ESI) mode at unit resolution. Electrospray capillary voltage was 3 kV, source temperature was 150 °C, and vaporizer temperature was 400 °C. Maximum desolvation gas (nitrogen) flow was applied, while the cone gas flow was switched off. Details on individual cone voltage, collision energy, and *m/z* transitions are given in Table 3. A dwell time of 30 ms was applied to all multiple reaction monitoring (MRM) transitions except to cyanidin for which this parameter was 50 ms. Unit resolution was adjusted on both quadrupoles.

RESULTS AND DISCUSSION

Method Development. The mass spectrometric behavior of all commercially available analytes was studied using both positive- and negative-ion ESI by direct infusion. Positive-ion ESI showed 2−3 times better sensitivity than negative-ion ESI, thus the positive mode was used for further work. Atmospheric pressure chemical ionization (APCI) exhibited approximately 50 times less intense signals compared to ESI. In positive-ion ESI, all target analytes yielded mass spectra dominated by the molecular ion (see mass spectrum of cyanidin 3-*O*-glucoside as an example in Figure 1A). $[M]^+$ is given as the identity of the molecular ion instead of $[M + H]^+$, since under acidic conditions anthocyanins exist as flavylium cations.[19] The magnified region shown as an insert in Figure 1A depicts the isotopomer distribution of the molecular ion. This shows how much signal is produced by an analyte 1, 2, or 3 amu higher than its monoisotopic mass. This latter aspect becomes important in cases where coeluting analytes occur in a wide dynamic range and the major constituents' (10^3−10^5 times more abundant than the minor ones) small but detectable signals appear in the channels of minor compounds that is 1, 2, and 3 amu higher in mass. Tandem mass spectrometric behavior of anthocyanins was then studied using collision-induced dissociation (CID). For maximized sensitivity and selectivity, the fragmentation of all analytes was optimized by recording product ion spectra at various collision energies in the 5−50 eV range. As an example, the fragmentation pattern of cyanidin 3-*O*-glucoside is shown in Figure 1B, where the loss of the sugar moiety (162 amu) dominates the pattern. While higher collision energies are used, several product ions with lower *m/z* values can be produced from anthocyanins, and the most intense transitions were clearly the ones reflecting the loss of sugar residues (glucose, rhamnose or rutinoside, sophoroside sugar units) and thus these were used in our further experiments. Table 3 shows the most intense transitions for all analytes in the present study.

Several solvent combinations were tested for optimal separation of the target analytes including water, ammonium-acetate buffer, acetonitrile, and methanol with different acidification levels. The presence of buffer resulted in adduct formation of analytes

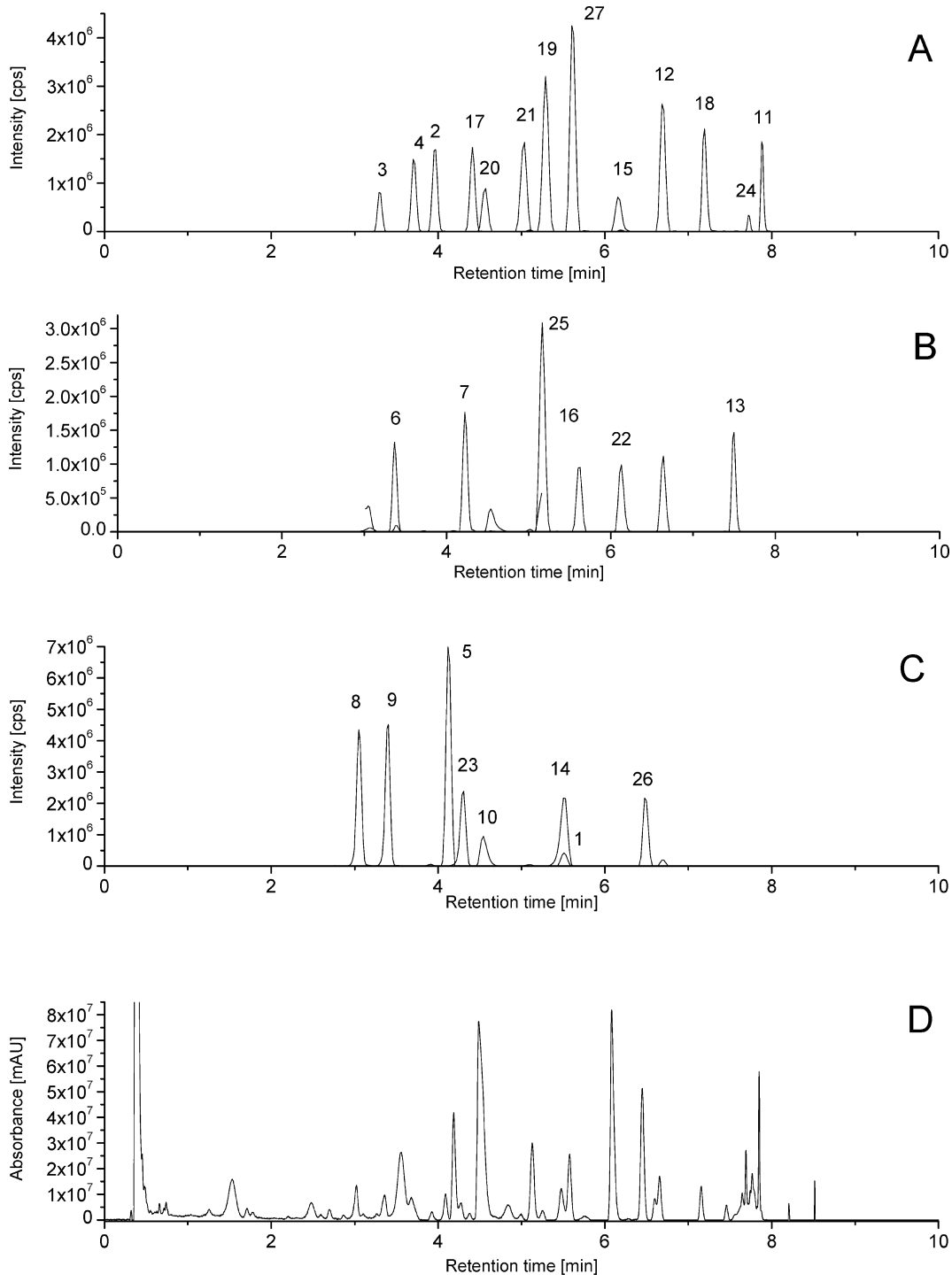

Figure 2. Reference UPLC−MS/MS and UV−VIS chromatograms obtained from a SMP sample enriched with anthocyanins and flavonols. The ion chromatograms are presented in three separate windows (A, B, C) in order to facilitate visualization. Peak identity is given by numbers, which correspond to analytes in Table 2. The chromatogram is 10 min long, and the whole run including equilibration is 13 min. Window D displays the obtained UV−VIS chromatogram from the same sample and same run. Note, that in the UV−VIS chromatogram, the separation is incomplete for most of the analytes, and since their UV−VIS profile is similar, the application of MS/MS is imperative for their distinct quantification.

compromising sensitivity and thus was not deployed. Separation power was similar between utilizing acetonitrile and methanol, but the observed pressure on the column was less with acetonitrile and thus this latter was employed in our further work. The best peak shape and separation power was achieved using an unusually acidic mobile phase (10% formic acid in mobile phase A, for details on the applied gradient profile see Table 1) on Ethylene Bridged Hybrid (BEH) C18 stationary phase. This phase is silica modified by trifunctional octadecyl chains and end-capping (particle size 1.7 μm, pore size 135 Å, carbon load 18%). While the biggest difference between this phase and conventional silica based octadecyl phases is the presence of ethylene bridges and reduced

Table 4. Validation Parameters Obtained for Anthocyanins in SMP Matrix

analyte	instrumental LLODs [ng/mL]	instrumental LLOQs [ng/mL]	fitted calibration	applied weighting	ng/mL of milk product	calibration fitting coefficient [R^2]	averaged accuracy [%]	recovery [%]	suppression [%]
cyanidin	60.0	200.0	quadratic	1/×2	600−60 000	0.976733	100	16	−88
cyanidin 3-*O*-arabinoside	2.0	6.0	linear	1/×2	12−36 000	0.990156	100	21	−35
cyanidin 3-*O*-galactoside	0.3	1.0	linear	1/×2	2−6 000	0.960567	100	26	−29
cyanidin-3-*O*-glucoside	0.3	1.0	linear	1/×2	2−6 000	0.993251	100	25	−30
cyanidin 3-*O*-rutinoside	3.0	10.0	linear	1/×2	20−60 000	0.992459	100	24	−26
cyanidin 3-*O*-sophoroside	1.0	3.0	linear	1/×2	6−18 000	0.978227	100	27	−27
delphinidin	300.0	1000.0	quadratic	1/×2	2 000−200 000	0.977392	99	17	−90
delphinidin 3-*O*-glucoside	3.0	10.0	linear	1/×2	20−60 000	0.993949	100	26	−36
delphinidin 3-*O*-rutinoside	3.0	10.0	linear	1/×2	20−60 000	0.995113	100	24	−29
ellagic acid	300.0	1000.0	quadratic	1/×	6 000−200 000	0.986089	95	70	−29
kaempferol	10.0	30.0	quadratic	1/×	30−90 000	0.992767	100	88	14
kaempferol 3-*O*-glucoside	10.0	30.0	quadratic	1/×	30−30 000	0.994073	104	60	−1
malvidin	20.0	60.0	quadratic	1/×2	180−18 000	0.960823	101	26	−94
malvidin 3-*O*-glucoside	2.0	6.0	linear	1/×	12−36 000	0.992063	100	27	−19
myricetin	10.0	30.0	quadratic	1/×2	30−3 000	0.964167	100	103	57
pelargonidin	10.0	30.0	quadratic	1/×2	90−27 0000	0.971727	98	15	−88
pelargonidin 3-O-glucoside	1.0	3.0	linear	1/×	18−18 000	0.990649	115	28	−35
peonidin	10.0	30.0	quadratic	1/×2	2 700−270 000	0.967595	101	27	−93
peonidin 3-*O*-arabinoside	1.0	3.0	quadratic	1/×2	9−27 000	0.981531	101	28	−46
peonidin 3-*O*-galactoside	1.0	3.0	linear	1/×	6−18 000	0.995848	101	27	−35
peonidin 3-*O*-glucoside	2.0	6.0	linear	1/×	12−36 000	0.992872	100	27	−36
petunidin	300.0	1000.0	quadratic	1/×2	6 000−600 000	0.973047	100	30	−89
petunidin 3-*O*-glucoside	2.0	6.0	linear	1/×	12−36 000	0.9935	100	28	−26
quercetin	20.0	60.0	linear	1/×2	60−6000	0.983662	100	89	2
quercetin 3-*O*-galactoside	20.0	60.0	quadratic	1/×	60−180−000	0.993123	107	60	−17
quercetin 3-*O*-rhamnoside	30.0	100.0	linear	1/×	100−30 000	0.973162	105	68	−24
quercetin 3-*O*-rutinoside	20.0	60.0	quadratic	1/×	60−180 000	0.987571	109	63	−10

number of free silanol groups, the number of this latter is still significant and contributes to the separation mechanism. On the basis of this, the authors propose that the separation mechanism is based on two major interactions: (1) apolar−apolar interaction between the analyte and octadecyl chains and (2) ionic interaction between the positive charge of the anthocyanin aglycone and negative charge of the dissociated silanol group. By application of very low pH (<2), the dissociation of silanol groups is efficiently suppressed hereby reducing the ionic interactions between analytes and stationary phase that are responsible for the peak asymmetry. This was confirmed by chromatograms (data not shown) that show strong peak fronting at pH ∼4 or higher and sharp, symmetric peaks at pH ≤ 2. The chemical resistance of BEH (applicable pH range 1−12) and the stability of the trifunctional C18 groups make this stationary phase the optimal choice for separation of anthocyanins at low pH. The final gradient was obtained by speeding up the chromatographic separation to a level where the isomeric glucoside and galactoside forms and other compounds with the same MRM transitions (such as ellagic acid and delphinidin) were still separated in order to enable their distinct quantification.

Chromatography dependent mass spectrometric parameters such as desolvation gas flow rate, desolvation gas temperature, and cone gas flow rate were optimized stepwise manually. A typical chromatogram for a mixture of 27 analytes is shown in Figure 2. Because of the high number of quantified analytes, the ion chromatograms are shown in three separate windows (A, B, C) to aid visibility and recognition of peaks. The identities of the peaks are given in Table 2. Retention time of the first analyte (delphinidin 3-*O*-glucoside) is 3.1 min, which ensures a good separation from the non- or weakly retained interferences such as vitamin C (antioxidant, used to protect analytes during the sample preparation process), which elutes around 0.4 min as confirmed by UV−VIS detection (see Figure 2D). The amount of the respective analytes corresponds to their 300 × LLOQ values, except for aglycones for which the 60 × LLOQ values correspond. In these chromatograms, the peak height was magnified by a factor of 10 for the analytes cyanidin, delphinidin, malvidin, myricetin, and petunidin in order to facilitate visualization among the other analytes. The reason for this measure is that the anthocyanins ionize approximately 10−100 times more efficiently than their aglycone counterparts due to the presence of the sugar moieties (see structure in Figure 1). This phenomenon is quantitatively reflected by the experimentally determined lower limits of quantification (LLOQ) for analytes with and without the sugar parts, as shown in Table 4. The recorded UV−VIS chromatogram (trace D in Figure 2) for the same sample is also given in order to illustrate how much tandem mass spectrometry improves peak recognition and quantification compared to UV−VIS detection. If individual wavelengths are interrogated from the UV−VIS data, most target analytes have very similar absorbance spectra (with a 520 nm maximum[25−27]) and their quantification is still hindered by their interference unless their full chromatographic separation is achieved. This latter problem becomes particularly pressing if the dynamic range of the analytes is wide (>1 order of magnitude) and if the major components' tailing/fronting mask the minor analytes.

The unique selectivity of tandem mass spectrometry enables distinct quantification of most polyphenols in a wide dynamic range, except for a few isomers where both the precursor and product ions have the same m/z values. Combining tandem mass spectrometry with UPLC overcomes even this latter problem, since UPLC can resolve the isomer pairs such as illustrated in

(27) Chirinos, R.; Campos, D.; Betalleluz, I.; Giusti, M. M.; Schwartz, S. J.; Tian, Q.; Pedreschi, R.; Larondelle, Y. *J. Agric. Food Chem.* **2006**, *54*, 7089–7097.

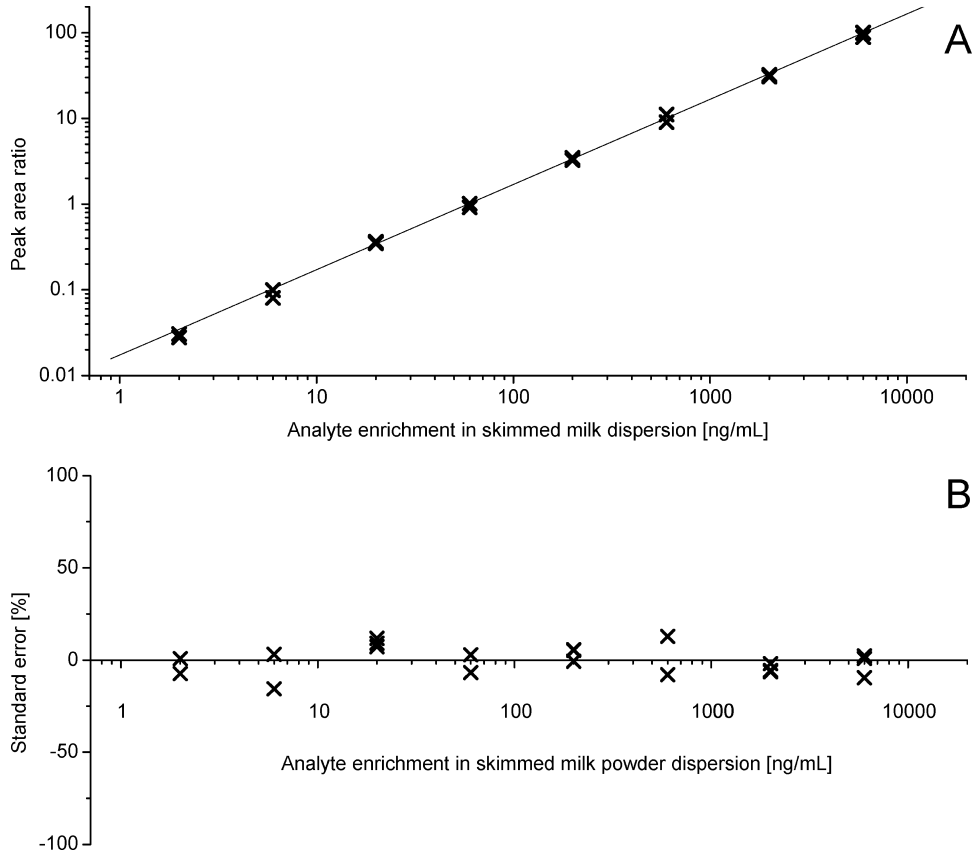

Figure 3. An example calibration curve (A) and residual plot (B) obtained for cyanidin 3-*O*-glucoside in SMP matrix. To aid visibility, the results are displayed on a logarithmic scale due to the wide concentration range covered (more than 3 orders of magnitude). Each calibration point represents separate sample preparation and thus includes the errors of the whole analytical process from sampling to peak integration.

the case of cyanidin 3-*O*-galactoside, -glucoside in Figure 2A. Therefore, UPLC−MS/MS represents a promising method of choice for studying anthocyanins and flavonols in highly complex samples and a wide dynamic range such as required for bioavailability and bioefficacy studies.

Method Validation. Skimmed milk powder (SMP) was selected as a model matrix to validate the method and to mimic matrix effects of milk-based food products during sample preparation and analysis. Prior to validation, the MRM channels of the internal standard (cyanidin 3-*O*-$^{13}C_6$-glucoside) were investigated in SMP to confirm the absence of interferences.

Instrumental lower limits of detection (LLODs; criterion, signal-to-noise >3) were determined by injecting dilution series of mixtures of all analytes. Lower limits of quantification (LLOQs; criterion, signal-to-noise >10) were determined in the same manner. Both LLOD and LLOQ results are shown in Table 4. As explained earlier, anthocyanidins (aglycones) exhibit higher LLOQs than anthocyanins. Calibration curves were established applying the method of standard additions using stock solutions A and B: the samples were spiked with known amounts of analytes before sample preparation. The spiking steps were adjusted for each analyte of stock solution A to be at the following levels: LLOQ, 3 × LLOQ, 10 × LLOQ, 30 × LLOQ, 100 × LLOQ, 300 × LLOQ, 1000 × LLOQ, 3000 × LLOQ. The spiking steps were adjusted for each analyte of stock solution B to be at the following levels: LLOQ, 3 × LLOQ, 6 × LLOQ, 10 × LLOQ, 30 × LLOQ, 60 × LLOQ, 100 × LLOQ. Each calibration point was determined in triplicate including the complete sample preparation step. Outliers were marked and excluded from the calibration process based on the following criteria: (1) the point deviates from the calibration curve by more than 30%; (2) on average two but a maximum of four points were excluded from the whole calibration process per each analyte (24 points altogether). Endogenous levels of analytes were not determined because the SMP matrix was found to be blank for the target analytes (for a given MRM pair at a given retention time window). A typical calibration curve is shown in Figure 3A for cyanidin 3-*O*-glucoside. The curve comprises a concentration range of 3 orders of magnitude starting from the LLOQ. Fitting coefficients and calibrated ranges for each analyte are shown in Table 4. While the quantitative range for most analytes was determined as 3 orders of magnitude, for some aglycones only narrower ranges (typically 2 orders of magnitude) could be achieved. The explanation for this latter is partly that these compounds (aglycones) exhibit 10 to 100 times lower ionization efficiency than others (glycosilated analytes) and partly that individual starting stock solution concentrations (before mixing with others) were close to the solubility limits, and this way the preparation of samples for calibration points at higher concentrations was not feasible.

Residual plots were also prepared and an example is shown in Figure 3B for cyanidin 3-*O*-glucoside. The plot illustrates in a normalized scale how the calibration points differ from the

Table 5. Intra- and Interday Precision Values at Two Different Concentration Levels[a]

analyte	intraday precision at 30 × LLOQ level [%] ($n = 7$)	intraday precision at 300 × LLOQ level [%] ($n = 7$)	interday precision at 30 × LLOQ level [%] ($n = 5$)	interday precision at 300 × LOQ level [%] ($n = 5$)
cyanidin	23.8	10.6	14.0	12.8
cyanidin 3-*O*-arabinoside	7.4	5.1	3.3	3.7
cyanidin 3-*O*-galactoside	6.4	7.8	8.0	0.9
cyanidin-3-*O*-glucoside	7.9	6.6	4.9	2.2
cyanidin 3-*O*-rutinoside	7.5	7.8	6.5	2.5
cyanidin 3-*O*-sophoroside	4.7	9.7	5.2	6.9
delphinidin	11.3	11.5	28.0	12.5
delphinidin 3-*O*-glucoside	6.0	8.0	3.5	3.2
delphinidin 3-*O*-rutinoside	5.8	6.9	4.2	4.2
ellagic acid	12.0	8.2	7.5	11.0
kaempferol	11.1	8.5	13.3	10.1
kaempferol 3-*O*-glucoside	9.7	8.7	8.8	5.5
malvidin	12.9	10.2	16.7	12.6
malvidin 3-*O*-glucoside	10.4	6.6	4.4	3.8
myricetin	11.4	13.0	15.9	35.2
pelargonidin	13.2	12.0	13.7	9.4
pelargonidin 3-O-glucoside	5.2	4.7	5.8	2.5
peonidin	13.0	10.7	16.6	12.2
peonidin 3-*O*-arabinoside	6.3	10.2	9.8	7.7
peonidin 3-*O*-galactoside	5.2	9.6	6.7	4.1
peonidin 3-*O*-glucoside	8.4	10.0	8.8	1.6
petunidin	20.7	13.5	19.0	5.3
petunidin 3-*O*-glucoside	8.8	6.0	7.2	2.2
quercetin	8.6	9.5	20.5	11.6
quercetin 3-*O*-galactoside	9.4	8.6	8.6	5.8
quercetin 3-*O*-rhamnoside	11.1	8.5	12.6	6.4
quercetin 3-*O*-rutinoside	7.7	5.8	5.4	3.2
average	9.8	8.8	10.3	7.4

[a] The data represent both the errors of sample preparation plus the errors of analytical detection.

Table 6. Anthocyanins and Flavonols Detected in Yogurt and Ice Cream Samples with Different Fruit Content

analyte	white grape yogurt [ng/mL]	strawberry yogurt [ng/mL]	plum yogurt [ng/mL]	apricot yogurt [ng/mL]	raspberry yogurt [ng/mL]	cherry yogurt [ng/mL]	strawberry ice cream [ng/mL]	apricot ice cream [ng/mL]
cyanidin						3501.9		
cyanidin 3-*O*-arabinoside	<LLOQ	<LLOQ	<LLOQ		107.7			
cyanidin 3-*O*-galactoside					171.2			
cyanidin-3-*O*-glucoside		322.4	65.9		882.1	>ULOQ	674.9	
cyanidin 3-*O*-rutinoside		28.3	2112.3		698.4	>ULOQ	70.4	
cyanidin 3-*O*-sophoroside		<LLOQ	6.1		13927.5	548.3	7.7	
delphinidin								
delphinidin 3-*O*-glucoside	<LLOQ	<LLOQ						
delphinidin 3-*O*-rutinoside	<LLOQ					<LLOQ	<LLOQ	
ellagic acid		11894.1			<LLOQ		16213.6	
kaempferol		49.6			<LLOQ	34.1	108.0	
kaempferol 3-*O*-glucoside	117.6	147.5	34.4		53.6	149.3	503.2	
malvidin								
malvidin 3-*O*-glucoside					<LLOQ			
myricetin							<LLOQ	
pelargonidin							431.5	
pelargonidin 3-O-glucoside	<LLOQ	16489.5	<LLOQ	<LLOQ	119.6	301.9	>ULOQ	<LLOQ
peonidin						<LLOQ		
peonidin 3-*O*-arabinoside				<LLOQ				
peonidin 3-*O*-galactoside								
peonidin 3-*O*-glucoside		<LLOQ	14.1		<LLOQ	303.7	<LLOQ	
petunidin								
petunidin 3-*O*-glucoside	<LLOQ							
quercetin	80.8	<LLOQ	72.8	<LLOQ	233.6	2965.9	669.1	
quercetin 3-*O*-rutinoside	65.6		5076.5	5842.1	<LLOQ	3670.7	143.4	536.1
quercetin 3-*O*-galactoside	<LLOQ		734.7		167.7		76.5	
quercetin 3-*O*-rhamnoside	<LLOQ		<LLOQ	<LLOQ				

calibration trend line and it aids in recognizing bending tendencies in the calibration (for wide concentration ranges usually "S-type" bending can be observed).

To investigate the efficacy of the sample preparation, the analyte recovery and ion suppression values were determined by comparing the peak areas between three types of samples: (1) SMP spiked before sample preparation with a known amount of analyte; (2) SMP spiked after sample preparation with a known amount of analyte; and (3) pure standard solution of analytes. The difference in peak areas between samples 2

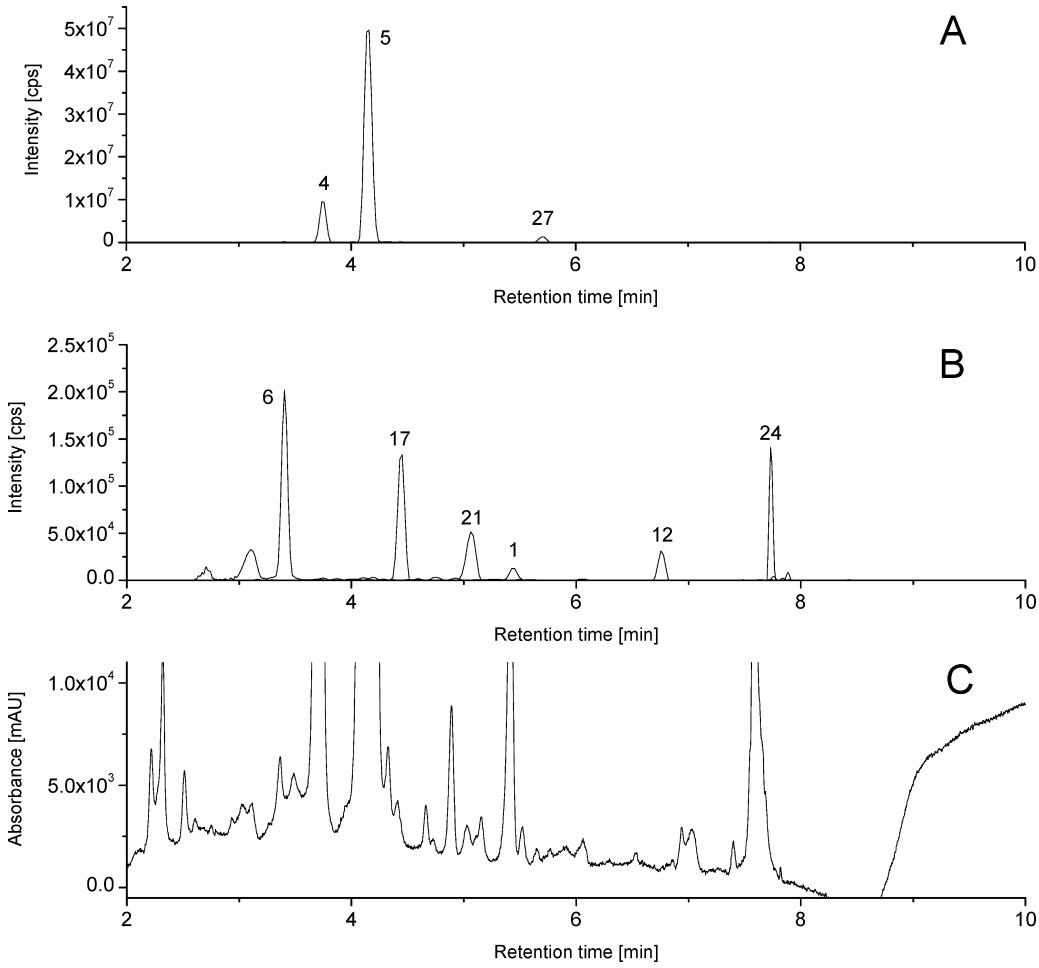

Figure 4. UPLC−MS/MS and UV−VIS chromatograms obtained from cherry yogurt. The ion chromatograms are presented in two separate windows (A, B) in order to facilitate visualization. Peak identity is given by numbers, which correspond to analytes in Table 2. Window C displays the obtained UV−VIS chromatogram from the same sample and same run. While in the UV−VIS chromatogram the separation is incomplete for most of the analytes, the MRM ion chromatograms contain well resolved, clean peaks enabling accurate quantification.

and 3 reflects the extent of ion suppression. The difference in peak areas between samples 1 and 2 reflects the recovery. Note that the reason for being able to calculate recovery this way is that the SMP is blank, does not contain endogenous anthocyanins. If the matrix contained endogenous analytes, then determination of recovery would require construction of calibrations by the method of standard additions before and after the sample preparation process in order to be able to calculate concentration of endogenous analytes. The two extraction steps at different pH (0 and 10% formic acid) have different effects on the recovery. Some analytes show better recovery utilizing only methanol as the extraction solvent (cyanidin 3-*O*-glucoside) while others are more efficiently recovered using acidified methanol (quercetin). Accordingly, combination of these two solvents was used to maximize overall recovery. Obtained recovery and suppression values for each analyte are given in Table 4. The accuracy (trueness) of the method was investigated by comparing theoretical and experimentally measured analyte levels, results are shown in Table 4.

Applications. The described method was applied to characterize the anthocyanin composition of yogurts and ice cream samples. Fruit yogurts and ice creams were obtained from the local grocery and were analyzed for their flavonoid content. Fruit contents on the product labels were specified as 9−10% for yogurts, 12% for apricot ice cream, and 19% for strawberry ice cream. Fat content was specified as 3% for apricot, strawberry, and cherry yogurt, while it was 0.1% (low fat) for grape, raspberry, and plum yogurts. Note, that in the case of ice cream, the measured flavonoid content corresponds to the composition of melted ice cream (frozen ice cream comprises 30−50% of air that escapes during melting). Determined concentrations are given in Table 6. While the profile of most dominant flavonoids is very different for the five yogurt types (for instance quercetin 3-*O*-rutinoside for plum, cyanidin 3-*O*-sophoroside for raspberry), also the minor anthocyanins differ very much in these samples. The results also reinforce our previous statement that while the MRM traces yield clean peaks which are easy to integrate, the UV−VIS trace shows strongly interfering peaks particularly if a major compound's tailing or fronting is superimposed on the signals of minor constituents. As an example, the flavonoid profile of cherry yogurt is given in Figure 4. On one hand, these observations suggest that the presented method is a promising approach for accurate determination of dietary anthocyanin intake in a wide dynamic range. On the other hand, these results emphasize that for nutritional intervention studies the accurate knowledge of anthocyanin content is crucial.

CONCLUSIONS

This manuscript describes and validates a comprehensive UPLC−MS/MS method combined with isotope dilution-based sample preparation for the quantitative analysis of anthocyanins and flavonols in milk-based food products. Methanol and acidified methanol are used as extraction solvents to precipitate the milk proteins and ultrafiltration is applied to separate target analytes from proteins. The UPLC separation enables short and efficient separation of isomers and reduction of suppression effects, while tandem mass spectrometric detection provides unique selectivity and sensitivity for quantifying 27 analytes in a wide dynamic range. To assess quantitative performance LLOD, LLOQ, linear range, precision, accuracy, and recovery were determined for the target analytes. Furthermore, the method was successfully applied to characterize the flavonoid content of yogurt and ice cream samples. The presented data suggest that this method will help better monitor dietary intake of anthocyanins and flavonols in bioavailability/bioefficacy studies, where health benefits of berry extracts in milk matrixes are studied.

ACKNOWLEDGMENT

K.N. and K.R. contributed equally to this manuscript. The authors would like to thank Prof. G. Williamson, Dr. J. Wang, Dr. F. Dionisi, Dr. Ph. Rousset, and Dr. B. Casado for the constructive consultations.

Received for review March 24, 2009. Accepted June 24, 2009.

AC900608G